European Commission | Funding & tender opportunities
Single Electronic Data Interchange Area (SEDIA)

H2020-MSCA-IF-2020

Secure Indoor Communication empowered by Intelligent reflecting Surface (SICIS)

D2.2

Report on joint beamforming optimization design for coordinating the transmission of multi-cell networks

Authors(s)	Sai Xu, Jiliang Zhang, Jie Zhang
Author(s) Affiliation	University of Sheffield, UK; University of Sheffield, UK; University of Sheffield, UK
Editor(s):	Sai Xu
Status-Version:	V1.0
Project Number:	101032170
Project Title:	Secure Indoor Communication empowered by Intelligent reflecting Surface
Project Acronym:	SICIS
Work Package Number	2

Abstract

This report investigates an intelligent reflecting surface (IRS) backscatter based uplink coordinated transmission strategy for a multi-cell network, where IRS serves as a transmitter enabling uplink transmission from each user to the associated base station (BS). To be specific, the considered network is made up of multiple cells, each of which consists of one multi-antenna BS and its served users. While one multi-antenna power beacon (PB) is deployed to radiate energy-bearing electromagnetic wave, the radio signal received by each IRS is modulated to send its connective user's information to the associated BS. Based on such a network framework, we maximize the weighted sum rate (WSR) under the constraints of total transmit power and reflecting coefficient by joint optimization of active beamforming at the PB, passive beamforming at the IRSs and uplink user scheduling. To address the problem, fractional programming (FP), alternative optimization and weighted bipartite matching are employed to convert the logarithm objective function into a more tractable form and to handle the optimization variables. The simulation results demonstrate the achievable WSR of the considered network.

The results presented in this deliverable have addressed the requirement of Task 2.2 in the SICIS project. The results are also a good reference for downlink multi-cell scenarios.

Keywords: Intelligent reflecting surface, reconfigurable intelligent surface, backscatter, uplink transmission, fractional programming, alternative optimization, weighted bipartite matching

Table of Contents

1. Introduction

In order to support an increasing number of user equipments (UEs), more and more base stations (BSs) are deployed in cellular systems [1]. Accompanied by highly dense BSs and UEs, excessive energy consumption for downlink and uplink wireless communications is caused. For the alleviation of this problem, green communications are always an active research area [2]. As a fully validated wireless technology, multiple-input multiple-output (MIMO), thanks to high degree of freedom resulting from spatial multiplexing, contributes to great improvement of energy efficiency (EE) [3]. Incorporating MIMO into cellular systems, the network capacity is raised drastically with high spectrum efficiency (SE) and EE. Additionally, multi-cell cooperation is often employed to effectively suppress co-channel interferences among multiple adjacent cells, thereby further facilitating EE [4], [5]. Although coordinated multi-cell MIMO has achieved considerable success, it is still not enough in reducing huge energy consumption of downlink and uplink transmissions between BSs and UEs, and how to implement fundamental improvement remains challenging.

Recently, intelligent reflecting surface (IRS) backscatter as an emerging paradigm has aroused rapidly growing interest, because of its ability to work as a low-power passive transmitter [6], [7]. Typically, IRS is a two-dimensional three-layer programmable metasurface, which consists of a control circuit board inside, a copper plate in the middle and a dielectric substrate outside [8]. On the substrate, a large number of low-cost passive reflecting elements are printed. When the incident signal reaches at each element, its electromagnetic (EM) characteristics, such as amplitude, phase, ect., can be changed in a real-time way [9]. Through collaboration, these elements can realize passive beamforming when the signal is reflected. Since no or few radio frequency (RF) chains are equipped, the power consumption of IRS is generally very low, compared to active antennas [10] and large intelligent surface (LIS) [11]. Therefore, IRS is positioned as an energy-effective enabler to promote wireless communications. On the other hand, backscatter is a technology, with which a device can remodulate the incoming signal to send its own data. During backscatter communications, the device does not transmit any RF signal. Instead, the incoming signal from other transmitters or wireless environment is harnessed to realize information transmission. Clearly, the energy consumption of communications at the device is eliminated by using the backscatter technology. As an integration of IRS and backscatter, IRS backscatter can reap the merits of the two techniques, thus mimicking transmit antennas in a passive way.

In this report, we will focus on the IRS backscatter based uplink coordinated transmission strategy for a radio cellular network. In this report, UEs in the network are considered to be immobile low-power Internet-of-Things (IoT) devices, each of which is linked to one IRS serving as a passive transmitter to enable uplink transmission. During uplink transmission, a dedicatedly-deployed power beacon (PB) is used to supply signal carrier for information modulation at each IRS, by radiating energy-bearing EM wave. Therefore, a UE is capable of sending its own information to the associated BS via IRS backscatter when scheduled for uplink transmission. Compared to conventional active antennas, the proposed network framework consumes lower transmit power at the UEs and has a lower hardware cost [8].

Currently, many existing works have demonstrated that it is feasible to employ IRS as a backscatter or transmitter to realize additional transmission. This report will focus on IRS backscatter based uplink coordinated transmission for a radio cellular network, distinguished from downlink communication in [12]. The main contents of this report are summarized as follows.

• This report investigates an IRS backscatter based uplink coordinated transmission framework for a radio cellular network, where IRS serves as a passive transmitter enabling uplink transmission from each UE to the associated BS. During uplink transmission, a dedicated PB is deployed to radiate

energy-bearing EM wave, while the radio signal received by each IRS is modulated to send its connective UE's information to the associated BS.

- Based on the established network framework, this report takes into account the maximization problem of WSR for uplink transmission under the constraints of total transmit power and reflecting coefficient. To address this challenging problem, fractional programming (FP), alternative optimization and weighted bipartite matching are employed to convert the logarithm objective functions into a more tractable form and to handle the optimization variables. Then, active beamforming at the PB, passive beamforming at the IRSs and uplink user scheduling are jointly optimized.
- Extensive simulations are executed to show the relationship between the achievable WSR of system and some important parameters, including the element number of IRS, the total transmit power at the PB, the antenna number of the BSs, the cell number, and the UE number of each cell. These results confirm the feasibility of the proposed IRS backscatter based uplink coordinated transmission strategy.

2. System Model and Problem Formulation

2.1. System Model

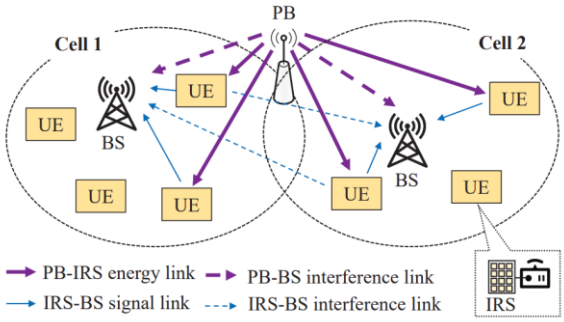

Fig. 1. An illustration of IRS backscatter based uplink coordinated multi-cell MIMO network model.

Consider an IRS backscatter based uplink coordinated multi-cell MIMO network, as illustrated in Fig. 1. In such a network, each cell consists of one BS and multiple UEs served by it. Each UE is linked to one IRS, thereby being capable of sending its own information to the associated BS via IRS backscatter when scheduled for uplink transmission. During uplink transmission, a dedicatedly-deployed PB is used to supply signal carrier for information modulation at each IRS, by radiating energy-bearing EM wave. In this network, IRS acts as a passive transmitter instead of a typical signal reflection device. It is assumed that all involved channels remain the same during any one of considered time blocks of interest, but may change over different ones. Other assumptions are that CSI is perfectly acquired for all transmission links, and that the channel and control information is available to the PB, the BSs and all the UEs.

In this network, the notations $\mathcal{I} = \{1, 2, \cdots, I\}$ and $\mathcal{K}_i = \{1, 2, \cdots, K_i\}$ are used to denote the sets of BSs (or cells) and UEs served by the *i*-th BS, respectively. Assume that all BSs and all IRSs have uniform hardware configuration, where each BS is equipped with N antennas and each IRS has L elements with the element set denoted by $\mathcal{L} = \{1, 2, \cdots, L\}$ }. In a time slot, each cell can support up to N UEs for simultaneous uplink transmission, owing to spatial multiplexing brought by multiple antennas. For the *i*-th cell, the variable $s_{in} \in \mathcal{K}_i$ is introduced to represent the index of the UE who is scheduled in the *n*-th stream at its BS. Additionally, the PB equipped with M antennas serves the scheduled UEs for their IRS backscatter. Note that if a UE is not scheduled to communicate with its associated BS, its linked IRS is turned into the completely absorbing mode, thereby generating no interference with the BSs.

Let $\mathbf{H}_{s_{in}} \in \mathbb{C}^{L\times M}$, $\mathbf{F}_{j,s_{in}} \in \mathbb{C}^{N\times L}$ and $\mathbf{G}_j \in \mathbb{C}^{N\times M}$ denote the channel gain matrices from the PB to the s_{in}-th UE, from the s_{in}-th UE to the *j*-th BS, and from the PB to the *j*-th BS, respectively. When the PB emits EM wave towards scheduled UEs in a time slot, the energy-bearing signal arriving at the IRS is recast to carry new data through modulation. Mathematically, the modulation process at the s_{in}-th IRS, if the corresponding UE is scheduled, is given by

$$\mathbf{F}_{j,s_{in}}\boldsymbol{\Theta}_{s_{in}}\mathbf{H}_{s_{in}}\mathbf{w}s = \mathbf{T}_{j,s_{in}}\boldsymbol{\theta}_{s_{in}}s \xrightarrow{\text{modulate}} \mathbf{T}_{j,s_{in}}\mathbf{v}_{s_{in}}x_{s_{in}},$$

where s and x_{sin} denote the original data from the PB and the modulated data from the s_{in} -th user, with $|s|^2 = 1$ and $E[|x_{sin}|^2] = 1$, respectively . The vector w represents the beamformer at the PB. θ_{sin} denotes the beamforming vector for the signal s. It is easy to find that $\mathbf{T}_{j,s_{in}} \triangleq \mathbf{F}_{j,s_{in}}\text{diag}\{\mathbf{H}_{s_{in}}\mathbf{w}\}$ and $\boldsymbol{\Theta}_{s_{in}} \triangleq \text{diag}\{\boldsymbol{\theta}_{s_{in}}\}$. From θ_{sin}s to v_{sin} x_{sin}, the signal modulation at IRS is fulfilled and $\mathbf{v}_{s_{in}}$ can be

viewed as the passive beamforming vector for the signal x_{sin} . Hence, $\left[\mathbf{v}_{s_{in}}\mathbf{v}_{s_{in}}^H\right]_{l,l} \leq 1$ holds, considering that the element reflection coefficient at IRS is not more than one.

Based on this network model, the received signal at the j-th BS is given by

$$\mathbf{y}_j = \sum_{(i,n)} \mathbf{T}_{j,s_{in}} \mathbf{v}_{s_{in}} x_{s_{in}} + \mathbf{G}_j \mathbf{w} s + \mathbf{n}_j,$$

where $\mathbf{n}_j$ is independent and identically distributed (i.i.d.) circularly symmetric complex Gaussian random vector with $\mathbf{n}_j \sim (0, \sigma^2 \mathbf{I})$. Then, the resulting SINR of the s_{in} -th data stream at the i-th BS is given by

$$\gamma_{i,s_{in}} = \mathbf{v}_{s_{in}}^H \mathbf{T}_{i,s_{in}}^H \left(\sigma^2 \mathbf{I} + \mathbf{G}_i \mathbf{w}\mathbf{w}^H \mathbf{G}_i^H + \sum_{(j,r)\neq(i,n)} \mathbf{T}_{i,s_{jr}} \mathbf{v}_{s_{jr}} \mathbf{v}_{s_{jr}}^H \mathbf{T}_{i,s_{jr}}^H \right)^{-1} \mathbf{T}_{i,s_{in}} \mathbf{v}_{s_{in}}.$$

Thus, the transmission rate from the s_{in} -th UE to the i-th BS is given by $R_{i,s_{in}} = \log\left(1 + \gamma_{i,s_{in}}\right)$.

2.2. Problem Formulation

Based on the aforementioned model, we aim to maximize the WSR of uplink transmission under the constraints of total transmit power and reflecting coefficient by joint optimization of active beamforming at the PB, passive beamforming at the IRSs and uplink user scheduling, which is formulated as

$$\begin{aligned} (\mathrm{P0}) \quad \max_{\mathbf{w},\mathcal{V},\mathcal{S}} \quad & \sum_{(i,n)} \omega_{i,s_{in}} R_{i,s_{in}}, \\ s.t. \quad & \mathrm{C1}: \mathrm{Tr}\left(\mathbf{w}\mathbf{w}^H\right) \leq P, \\ & \mathrm{C2}: \left[\mathbf{v}_{s_{in}}\mathbf{v}_{s_{in}}^H\right]_{l,l} \leq 1, \ l \in \mathcal{L} \\ & \mathrm{C3}: s_{in} \in \mathcal{K}_i \cup \{\varnothing\}, \end{aligned}$$

where V and S refer to the collections of v_{sin} and s_{in}, respectively. The weighting factor $\omega_{i,s_{in}}$ accounts for the priority of the s_{in}-th UE at the i-th BS. P denotes the allowable maximum transmit power overhead of the PB. Note that the allowable maximum number of scheduled UEs per cell is N, which is bounded by the antenna number of each BS.

3. Uplink WSR Maximization

The problem (P0) is challenging to address directly, since the optimization variables w, v_{sin} , and s_{in} are deeply coupled and the objective function is in a form of weighted sum of logarithm functions. To handle the problem (P0), this section will firstly employ Lagrangian dual transform, being a typical method of FP, to convert the objective function into a new form. Then, alternative optimization and weighted bipartite matching are adopted to optimize w, v_{sin} and s_{in}. Finally, the computational complexity is analyzed.

3.1. Objective Function Conversion

The objective function of the problem (P0) is in a form of weighted sum of logarithm functions. To make the problem (P0) more tractable, Lagrangian dual transform is leveraged to convert the objective function into a new form. Specifically, introducing auxiliary variable $\alpha_{s,in}$, the weighted sum of logarithm functions is transformed into

$$\begin{aligned}\sum_{(i,n)} \omega_{i,s_{in}} R_{i,s_{in}} &= \sum_{(i,n)} \omega_{i,s_{in}} \log\left(1+\gamma_{i,s_{in}}\right) \\ &= \max_{\alpha_{i,s_{in}} \geq 0} \sum_{(i,n)} \omega_{i,s_{in}} \left[\log\left(1+\alpha_{i,s_{in}}\right) - \alpha_{i,s_{in}}\right] \\ &\qquad + \frac{\omega_{i,s_{in}}\left(1+\alpha_{i,s_{in}}\right)\gamma_{i,s_{in}}}{1+\gamma_{i,s_{in}}}.\end{aligned}$$

Using quadratic transform, we have

$$\begin{aligned}\frac{\omega_{i,s_{in}}\left(1+\alpha_{i,s_{in}}\right)\gamma_{i,s_{in}}}{1+\gamma_{i,s_{in}}} &= \frac{\omega_{i,s_{in}}\left(1+\alpha_{i,s_{in}}\right)\left|\mathrm{A}_{i,s_{in}}\right|^2}{\mathrm{B}_i} \\ =2\sqrt{\omega_{i,s_{in}}(1+\alpha_{i,s_{in}})}\mathrm{Re}\{\boldsymbol{\beta}_{i,s_{in}}^H \mathrm{A}_{i,s_{in}}\} &- \boldsymbol{\beta}_{i,s_{in}}^H \mathrm{B}_i \boldsymbol{\beta}_{i,s_{in}}\end{aligned}$$

where $\beta_{i,sin}$ is an auxiliary variable vector, and $A_{i,sin}$ and B_i are respectively given by

$$\begin{aligned}&\mathrm{A}_{i,s_{in}} = \mathbf{T}_{i,s_{in}} \mathbf{v}_{s_{in}}, \\ &\mathrm{B}_i = \sigma^2 \mathbf{I} + \mathbf{G}_i \mathbf{w}\mathbf{w}^H \mathbf{G}_i^H + \sum_{(j,r)} \mathbf{T}_{i,s_{jr}} \mathbf{v}_{s_{jr}} \mathbf{v}_{s_{jr}}^H \mathbf{T}_{i,s_{jr}}^H.\end{aligned}$$

Thus, the problem (P0) is reformulated as

$$\begin{aligned}(\mathrm{P1}) \quad \max_{\mathbf{w},\mathcal{V},\mathcal{S},\alpha,\boldsymbol{\beta}} \quad & f(\mathbf{w},\mathcal{V},\mathcal{S},\alpha,\boldsymbol{\beta}), \\ & \mathrm{C1}-\mathrm{C3}, \\ & \mathrm{C4}: \alpha_{i,s_{in}} \geq 0,\end{aligned}$$

where α and β refer to the collections of $\alpha_{i,sin}$ and $\beta_{i,sin}$, and

$$\begin{aligned}f(\mathbf{w},\mathcal{V},\mathcal{S},\alpha,\boldsymbol{\beta}) \triangleq & \sum_{(i,n)} \omega_{i,s_{in}} \left[\log\left(1+\alpha_{i,s_{in}}\right) - \alpha_{i,s_{in}}\right] \\ & + 2\sqrt{\omega_{i,s_{in}}(1+\alpha_{i,s_{in}})}\mathrm{Re}\{\boldsymbol{\beta}_{i,s_{in}}^H \mathrm{A}_{i,s_{in}}\} - \boldsymbol{\beta}_{i,s_{in}}^H \mathrm{B}_i \boldsymbol{\beta}_{i,s_{in}}.\end{aligned}$$

Since the optimization variables w, v_{sin} , and sin are deeply coupled in the constraints, the problem (P1) is still challenging to solve directly. In the following subsection, we will present an alternative optimization method to solve the problem (P1).

3.2. Alternative Optimization

This subsection will provide an alternative optimization procedure to address the problem (P1) by cyclically optimizing the variables α, β, w, V and S, which is divided into three step.

Step-1): Optimizing α and β

Given w, V, and S, we separately take a derivative with respect to $\alpha_{i,sin}$ and $\beta_{i,sin}$ to obtain the optimal $\alpha^\circ_{i,sin}$ and $\beta^\circ_{i,sin}$. Mathematically, let

$$\frac{\partial f(\mathbf{w},\mathcal{V},\mathcal{S},\alpha,\boldsymbol{\beta})}{\partial \alpha_{i,s_{in}}} = 0,$$
$$\frac{\partial f(\mathbf{w},\mathcal{V},\mathcal{S},\alpha,\boldsymbol{\beta})}{\partial \boldsymbol{\beta}_{i,s_{in}}} = 0.$$

It is derived that the optimal $\alpha^\circ_{i,sin}$ and $\beta^\circ_{i,sin}$ are respectively given by

$$\alpha^{\circ}_{i,s_{in}} = \gamma_{i,s_{in}},$$
$$\boldsymbol{\beta}^{\circ}_{i,s_{in}} = \sqrt{\omega_{i,s_{in}}(1+\alpha_{i,s_{in}})}\mathrm{B}_i^{-1}\mathrm{A}_{i,s_{in}}.$$

Step-2): Optimizing w

To make the problem (P1) tractable, semidefinite relaxation (SDR) is performed to lift (P1) into a higher dimension. Then, this problem (P1) is equivalently rewritten as

$$\begin{aligned}
(\mathrm{P2}) \quad \min_{\hat{\mathbf{W}}} \quad & \sum_{(i,n)} \mathrm{Tr}\left(\mathbf{Y}_{i,s_{in}}\mathbf{W}\right) - \mathrm{Tr}\left(\mathbf{X}_{i,s_{in}}\hat{\mathbf{W}}\right), \\
s.t. \quad & \mathrm{C5}: \mathrm{Tr}\left(\mathbf{W}\right) \le P, \\
& \mathrm{C6}: \left[\hat{\mathbf{W}}\right]_{M+1,M+1} = 1, \\
& \mathrm{C7}: \hat{\mathbf{W}} \succeq \mathbf{0}, \\
& \mathrm{C8}: \mathrm{rank}\left(\hat{\mathbf{W}}\right) = 1.
\end{aligned}$$

Dropping the constraint C8, the problem (P2) is relaxed as a convex semidefinite program (SDP) problem and can be addressed by existing CVX solvers. Then, the rank-one solution w° can be recovered by using singular value decomposition (SVD) if the rank of the optimal W° is one. Otherwise, the Gaussian randomization method may be used to recover the rank-one solution w° or the eigenvector corresponding to the maximum eigenvalue of W° is approximately used as w°

Step-3): Optimizing V and S

Given w, α and β, the problem (P1) is reformulated as

$$\begin{aligned}
(\mathrm{P3}) \quad \max_{\mathcal{V}} \quad & \sum_{(i,n)} \Bigg[\sqrt{\omega_{i,s_{in}}(1+\alpha_{i,s_{in}})}\mathrm{Tr}(\boldsymbol{\Omega}_{i,s_{in}}\hat{\mathbf{V}}_{s_{in}}) \\
& \qquad - \sum_{(j,r)} \mathrm{Tr}\left(\boldsymbol{\beta}_{i,s_{in}}\boldsymbol{\beta}^H_{i,s_{in}}\mathbf{T}_{i,s_{jr}}\mathbf{V}_{s_{jr}}\mathbf{T}^H_{i,s_{jr}}\right) \Bigg], \\
s.t. \quad & \mathrm{C4}: s_{in} \in \mathcal{K}_i \cup \{\varnothing\}, \\
& \mathrm{C9}: \left[\hat{\mathbf{V}}_{s_{in}}\right]_{l,l} \le 1, \ l \in \mathcal{L}, \\
& \mathrm{C10}: \left[\hat{\mathbf{V}}_{s_{in}}\right]_{L+1,L+1} = 1, \\
& \mathrm{C11}: \hat{\mathbf{V}}_{s_{in}} \succeq \mathbf{0}, \\
& \mathrm{C12}: \mathrm{rank}\left(\hat{\mathbf{V}}_{s_{in}}\right) = 1.
\end{aligned}$$

If the user scheduling S is given, the maximum uplink WSR can be acquired by cyclically optimizing α, β, w, and V. When the number of cell UEs (i.e. UEs within a cell) is small, the optimal S° can be obtained by going through all the user scheduling cases. However, when the number of cell UEs is large, the ergodic user scheduling method has an extremely high computational complexity. Then, the problem (P3) for given $\xi_{sin,n}$ is simplified as a weighted bipartite matching problem as follows.

$$
\begin{aligned}
(\text{P3'}) \quad \max_{\mathcal{V}} \quad & \sum_{s_{in}\in\mathcal{K}_i}\sum_{n=1}^{N} x_{s_{in},n}\xi_{s_{in},n}, \\
s.t. \quad & \text{C13}: \sum_{s_{in}\in\mathcal{K}_i} x_{s_{in},n} \le 1, \\
& \text{C14}: \sum_{n=1}^{N} x_{s_{in},n} \le 1, \\
& \text{C15}: x_{s_{in},n} \in \{0,1\},
\end{aligned}
$$

4. NUMERICAL RESULTS

In this section, we will examine the feasibility and the communication performance for the proposed IRS backscatter based uplink coordinated multi-cell MIMO network by extensive numerical simulations, including the convergence behavior of the optimization schemes, how the element number at IRS, the transmit power budget at the PB, the antenna number of BSs, the cell number and the UE number of each cell affect the achievable WSR of system, and the robustness of the proposed optimization scheme. Besides the proposed optimization scheme, several other benchmark schemes are given for comparison.

Joint: This legend represents the proposed optimization scheme for the considered IRS backscatter based uplink coordinated multi-cell MIMO network, in which FP and alternative optimization are employed to convert the logarithm objective functions into a more tractable form and to handle the coupled optimization variables, as detailed in Section III.

Antenna4 and Antenna8: The two legends denote the optimization schemes for the conventional uplink coordinated multi-cell MIMO network, in which each UE employs active antennas (’4’ and ’8’ denote the antenna number) to communicate with BSs without the deployment of PB.

Passive: This legend represents a specific optimization scheme for the simplified IRS backscatter based uplink coordinated multi-cell MIMO network, in which the PB is removed and the reflection power at each IRS element is equal. For a fair performance comparison between IRS backscatter and active antennas, the reflection power at each IRS in Passive is set to be the same as active antennas in Antenna4 and Antenna8.

Discrete4 and Discrete8: The two legends denote the discrete optimization schemes for the considered IRS backscatter based uplink coordinated multi-cell MIMO network. The only difference of Discrete4 and Discrete8 (’4’ and ’8’ denote the number of discrete values) from Joint is that the passive beamforming at each IRS is discrete.

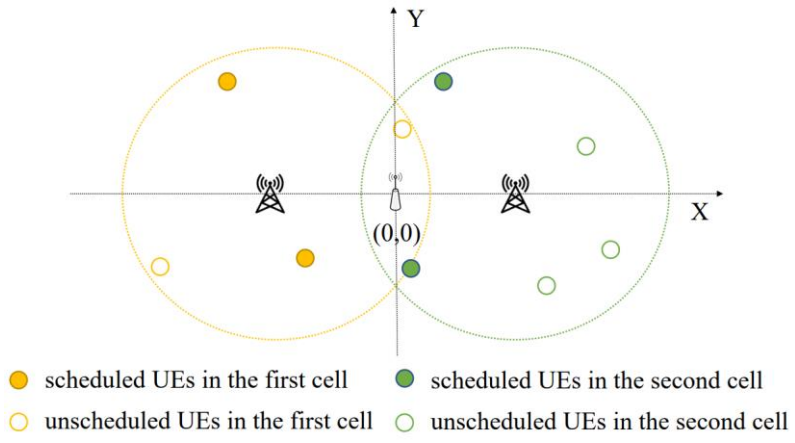

Fig. 2. Spatial distribution of PB, BSs and UEs.

In the numerical simulations, we consider Rician fading, with the Rician factor κ, for all involved channels. Let dx and d0 denote the transmission distance and the reference distance, respectively. Then, the path loss can be modelled as PL = PL0 − 25 lg (dx/d0) dB with PL0 = -30 dB. Generally speaking, the incoming signal is only reflected by the front half-sphere of IRS, and thus there exists a 3 dBi gain for the reflection. In Fig. 2, the spatial distribution of PB, BSs and UEs is shown, where the PB is deployed in the ordinate origin (0, 0) while two BSs with the same antenna number are located in the positions (-50, 0) and (50, 0), respectively. For simplicity, the UE number in each cell is identical and the positions of UEs are randomly and independently generated within the radius r of cell. In TABLE I, some important.

TABLE I Simulation Parameters

Notation	Description	Value
κ	Rician factor	3
d_0	Reference distance	1m
d	Distances from PB to BSs	50 m
r	Cell radius	60 m
I	Cell or BS number	2
K	UE number in single cell	2
M	Antenna number of PB	4
N	Antenna number of BSs	2
L	Element number of IRS	64
P	Total transmit power of PB	9 dBW
P_a	Transmit power of each active UE	3 dBm
σ^2	Noise variance	-94 dBm
ω_{jk}	Weighting factor	1

Fig. 3 shows the convergence behavior of the schemes of Joint, Passive, Antenna4 and Antenna8 for the uplink coordinated multi-cell MIMO network in a random observation. From Fig. 3, it is clearly observed that the schemes of Joint, Passive, Antenna4 and Antenna8 converge very quickly. When the iteration reaches five times, the achievable WSR tends to level off. By comparing Passive with Antenna4 and Antenna8, it can be found that the proposed framework of IRS backscatter gains a better communication performance. That is primarily because the element number of IRS is far more than the active antenna number, which brings a higher degree of spatial freedom.

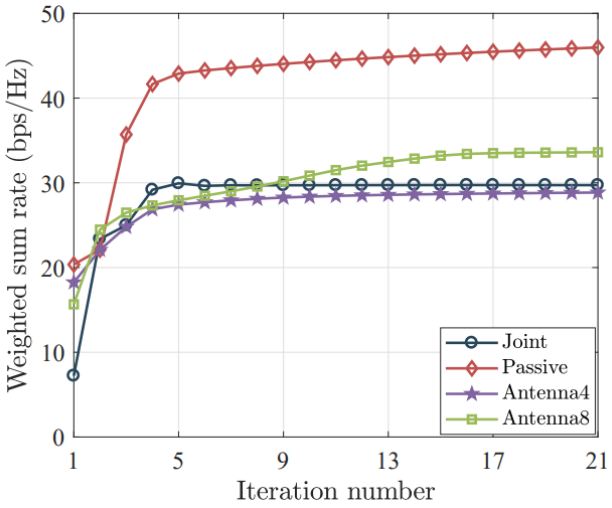

Fig. 3. Convergence behavior of the schemes of Joint, Passive, Antenna4 and Antenna8 for the uplink coordinated multi-cell MIMO network in a random observation.

Figs. 4 and 5 depict the impact of the element number of IRS and the total transmit power at the PB on the achievable WSR of system for the proposed IRS backscatter based uplink coordinated multi-cell MIMO network, respectively. Note that the total transmit power in Passive, Antenna4 and Antenna8 ranges from 3 dBm to 9 dBm, with the step length being 1 dBm. From Figs. 4 and 5, it can be seen that the achievable WSR of system is improved in the schemes of Joint, Passive, Discrete4 and Discrete8, when the number of elements on each IRS increases or higher total transmit power at the PB is utilized. For the schemes of Antenna4 and Antenna8, an increase in the total transmit power contributes to improving the achievable WSR of system.

By comparison, the scheme of Joint is slightly superior to Discrete4 and Discrete8, which indicates that the proposed IRS backscatter scheme can be applied to practical discrete phase and amplitude. On the other hand, the IRS backscatter scheme can be assessed by comparing the schemes of Antenna4 and Antenna8 with Passive. Among all these schemes, Passive achieves the maximum communication performance. Therefore, it can be concluded that a higher degree of spatial freedom owing to many IRS elements is beneficial to facilitating communication performance. It is worth mentioning that the huge energy loss of EM wave from the PB to the IRSs is an adverse factor, observing that Passive, with far lower total power consumption, outperforms Joint. This result implies that the deployment of PB is crucial to the network energy consumption.

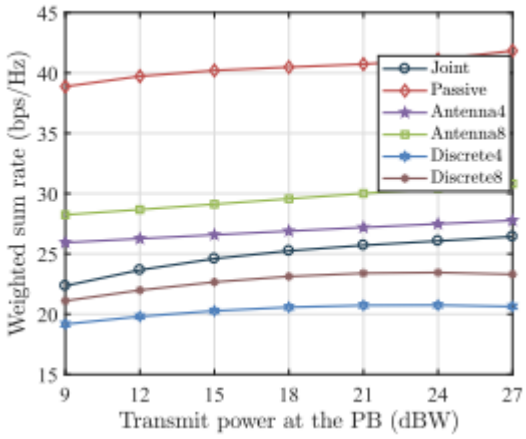

Fig. 4 The relationship between the total transmit power at the PB and the achievable WSR of system for the proposed IRS backscatter based uplink coordinated multi-cell MIMO network. Note that the total transmit power in Passive, Antenna4 and Antenna8 ranges from 3 dBm to 9 dBm, with the step length being 1 dBm

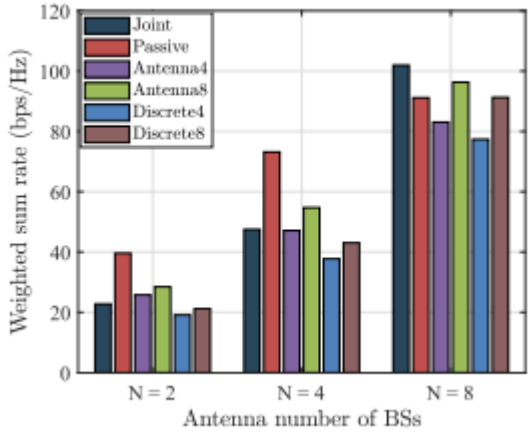

Fig. 5. The relationship between the antenna number of BSs and the achievable WSR of system for the proposed IRS backscatter based uplink coordinated multi-cell MIMO network.

Figs. 5, 6 and 7 depict the impact of the antenna number of BSs, the cell number, and the UE number of each cell on the achievable WSR of system for the proposed IRS backscatter based uplink coordinated multi-cell MIMO network. In the numerical simulations, when the cell number is set as I = 4, four BSs are positioned at (50, 0), (−50, 0), (0, 50), and (0, −50), respectively. If I is less than four, any I positions are selected from them to place the BSs. From these simulation figures, it is seen that an increase in the antenna number of BSs, the cell number, and the UE number of each cell can increase the achievable WSR of system. The reasons are summarized as follows: 1) When the BSs are equipped with more antennas, more data streams and more cell UEs can be supported for simultaneous uplink transmission in a cell; 2) When more BSs are deployed to form more cells, more energy from the PB can be harvested and more UEs can be scheduled to access wireless network; 3) When more UEs of each cell exist, the degree of spatial freedom is improved. These simulation results further verify that the proposed IRS backscatter based uplink coordinated multi-cell MIMO network is feasible.

5. Conclusion

The focus of the research presented an IRS backscatter based uplink coordinated transmission strategy for a radio cellular network. In this network, we investigated the WSR maximization problem and employed the methods of FP, alternative optimization and weighted bipartite matching to solve it. By simulations, it was verified that an increase in the element number of IRS, the total transmit power at the PB, the antenna number of the BSs, the cell number, and the UE number of each cell contributes to improving the achievable WSR of system. In addition, it was verified that the proposed optimization scheme had a good robustness, especially in the case of large noise variance. On the other hand, like conventional uplink coordinated transmission framework in which the UEs were equipped with active antennas, the proposed paradigm of IRS backscatter achieved a satisfactory WSR of system with consuming the same transmission power. These result confirmed the feasibility of the proposed IRS backscatter based uplink coordinated transmission strategy..

References

1. S. Chen, T. Zhao, H.-H. Chen, and W. Meng, "Network densification and path-loss models versus UDN performance—A unified approach," *IEEE Trans. Wireless Commun*., vol. 20, no. 7, pp. 4058–4071, Jul. 2021.
2. S. Buzzi, I. Chih-Lin, T. E. Klein, H. V. Poor, C. Yang, and A. Zappone, "A survey of energy-efficient techniques for 5G networks and challenges ahead," *IEEE J. Sel. Areas Commun*., vol. 34, no. 4, pp. 697–709, Apr. 2016.
3. D. Gesbert, S. Hanly, H. Huang, S. S. Shitz, O. Simeone, and W. Yu, "Multi-cell MIMO cooperative networks: A new look at interference," *IEEE J. Sel. Areas Commun*., vol. 28, no. 9, pp. 1380–1408, Dec. 2010.
4. M. Hua, Q. Wu, D. W. K. Ng, J. Zhao, and L. Yang, "Intelligent reflecting surface-aided joint processing coordinated multipoint transmission," *IEEE Trans. Commun*., vol. 69, no. 3, pp. 1650–1665, Mar. 2021.
5. R. Zhang, "Cooperative multi-cell block diagonalization with per-basestation power constraints," *IEEE J. Sel. Areas Commun*., vol. 28, no. 9, pp. 1435–1445, Dec. 2010.
6. S. Xu, J. Liu, T. K. Rodrigues, and N. Kato, "Envisioning intelligent reflecting surface empowered space-air-ground integrated network," *IEEE Netw*., vol. 35, no. 6, pp. 225–232, Nov. 2021.
7. S. Xu, J. Liu, Y. Cao, J. Li, and Y. Zhang, "Intelligent reflecting surface enabled secure cooperative transmission for satellite-terrestrial integrated networks," *IEEE Trans. Veh. Technol*., vol. 70, no. 2, pp. 2007–2011, Feb. 2021.
8. Q. Wu and R. Zhang, "Towards smart and reconfigurable environment: Intelligent reflecting surface aided wireless network," *IEEE Commun. Mag*., vol. 58, no. 1, pp. 106–112, Jan. 2020.
9. M. Di Renzo et al., "Smart radio environments empowered by reconfigurable intelligent surfaces: How it works, state of research, and the road ahead," *IEEE J. Sel. Areas Commun*., vol. 38, no. 11, pp. 2450–2525, Nov. 2020.
10. C. Huang et al., "Holographic MIMO surfaces for 6G wireless networks: Opportunities, challenges, and trends," *IEEE Wireless Commun.*, vol. 27, no. 5, pp. 118–125, Oct. 2020.

11. S. Hu, F. Rusek, and O. Edfors, "Beyond massive MIMO: The potential of data transmission with large intelligent surfaces," *IEEE Trans. Signal Process.*, vol. 66, no. 10, pp. 2746–2758, May 2018.
12. S. Xu, Y. Du, J. Liu, and J. Li, "Weighted sum rate maximization in IRS BackCom enabled downlink multi-cell MISO network," *IEEE Commun. Lett.*, vol. 26, no. 3, pp. 642–646, Mar. 2022.